



# Numerical Investigation Of Reinforced Concrete Coupled Shear Walls With Replaceable Steel Fuses

<sup>1</sup>Amr Magdy, <sup>2</sup>Ali Hammad, <sup>3</sup>Hussein Okail, <sup>3</sup>Marwan Shedid

<sup>1</sup>Teaching Assistant, <sup>2</sup>Assistant Professor, <sup>3</sup>Professor  
Structural Engineering Department,  
Ain Shams University, Cairo, Egypt

**Abstract:** Structural fuses are sacrificial structural elements that can be added to Reinforced Concrete (RC) systems to reduce the damage under seismic loads. Coupled shear walls system is chosen in this research to be studied while installing steel fuse coupling beams with specific recommendations instead of conventional concrete beams. Many studies investigated the shear behavior of steel beams under shear loading, and others applied lateral loading on coupled shear walls with steel beams. A non-linear finite element analysis is conducted using ABAQUS FE program to verify the modeling of steel fuse beams under shear loading, and Seismostruct FE program is used to verify modeling of global reinforced concrete system under lateral loads based on available experimental results. The numerical results were found reliable to simulate the behavior of verified specimens. Then, a parametric study is conducted using the verified micro and macro modelling technique through two phases; phase one aims to determine the optimum dimensions for steel fuse coupling beams to enhance its performance in terms of shear-deformation capacity, and energy absorption ensuring shear yielding instead of flexural yielding, while the second phase aims to study the effect of installing steel beams with the design guidelines deduced from phase one instead of conventional RC beams and predict the effect of this procedure on the global behavior of the main system including base shear capacity, ultimate top displacement, and energy dissipation. In conclusion, a specific factor range is identified for steel beams to ensure better shear behavior. Additionally, RC coupled wall systems with steel coupling beams showed better performance in terms of ductility, energy dissipation, and damages level while maintaining similar shear capacity compared to the ordinary systems coupled with RC beams.

**Keywords:** Coupled shear walls; Structural fuses; Steel link beams; Finite element modeling; Hysteresis behavior

## 1. INTRODUCTION

The field of structural systems seismic design has made significant strides in recent decades, focusing on cost reduction in construction and repair of various structures including buildings, bridges, and factories. Ensuring the serviceability of these structures after strong earthquakes has become a crucial objective, particularly for bridges and factories that needs to remain operational during and right after seismic events. To reduce the initial construction costs, reduction factors were introduced for seismic design forces, considering system ductility. However, this approach led to high repair costs and the potential for buildings to go out of service after intense earthquakes. It also resulted in damage to main structural elements, leading to structural collapse and loss of life in some cases. To address these concerns, the concept of structural fuses was introduced. Fuses are defined as sacrificial elements strategically placed to protect other main structural elements, such as walls and columns to ensure safety during and after an extreme event. Fuses are positioned at points of high shear or rotational deformation which can concentrate stresses in ductile materials like steel, dissipating seismic energy while preserving the strength of the main reinforced concrete elements.

Previous studies explored various forms of structural fuses. Roeder and Popov 1977 [1] introduced eccentric braced steel frames (EBFs), which focused seismic damage in the eccentric part of horizontal beams between diagonal braces, utilizing their ductility to protect the main frame and braces. However, Fintel and Ghosh 1981 [2] has studied approaches like weak beam-strong column concepts. The common thing between these concepts is that they reduced initial construction costs but resulted in high repair costs and duration.

To mitigate repair duration and operational disruptions, replaceable structural fuses were later introduced. This leads to localized damage within specific elements that can be easily replaced after extreme events. Experimental tests done by Fortney et al. [3] on steel beams with replaceable weak bolted intermediate parts demonstrated their effectiveness. Further studies investigated coupled shear walls with concrete and steel coupling beams, showing reduced damage in systems incorporating steel fuses (Chen, 2019 [4]; Cheng, 2015 [5]; Li et al [6] ).

This study aims to extend the investigation of replaceable fuses in reinforced concrete coupled wall seismic resisting systems using numerical modeling. Finite element models are verified against previous experiments to ensure reliability. Then, a parametric study examines different parameters to understand seismic behavior and investigate global behavior, including maximum displacement, base shear, energy dissipation, and damage sequence. Additionally, steel fuse beams with different designs and dimensions are studied under shear loading to recommend ideal conditions based on rotational ductility and capacity.

## 2.FINITE ELEMENT MODELING

### 2.1 Finite Element Program

Steel fuse beams are modeled individually to study the shear behavior and stress distribution along the beams under point shear vertical deformation at one end while fixing the other beam end. The modeled steel beam end conditions are chosen to simulate previous shear test to deduce the coupled beam behavior in shear wall systems. Coupled shear wall systems are modeled to study the global system behavior and damage sequence. Walls bases are fixed at the bottom, and laterally loaded from the top by cyclic quasi-static record.

ABAQUS Finite Element (FE) software [7] is employed to model the steel fuse beams and extract important shear behavior parameters, including initial stiffness, yield shear force, yield displacement, peak shear force, and peak displacement. These parameters are then utilized to define the shear spring properties of the steel fuse link element in the global system model.

To simulate the behavior of the entire reinforced concrete (RC) system, specifically the coupled shear wall, under lateral cyclic loading, the SeismoStruct FE software [8] is utilized.

### 2.2 Steel Beams Modeling

A steel bi-linear model is implemented in ABAQUS FE to define the stress-strain characteristics of the steel beams material. To determine the shear parameters for the steel beams, one end of each beam is fixed using an “Encaster” boundary condition, while the other end is vertically loaded with a point load. The loaded end of the beam is subjected to boundary conditions that don’t allow rotation about the x and z axes, ensuring pure shear behavior. The steel beam elements are modeled using 8-node integrated solid elements (C3D8R) to prevent shear locking under bending moments. The Arc-Length method is employed for displacement-controlled shear loading of the steel beams through static-riks analysis. The meshing size of the steel beam elements is set to 5mm after conducting several trials to ensure accurate results and minimize analysis time. It should also be noted that ABAQUS is selected due to its capability to simulate shear deformations in small elements. **Fig. 1** shows steel beam modeling conditions in FE software.

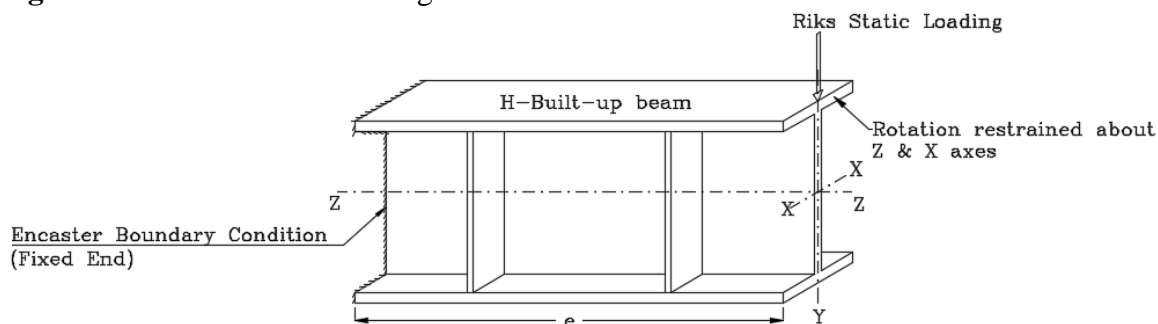


**Fig. 1** Steel Beam Modeling Conditions

### 2.3 Coupled Shear Wall Modeling

The seismic response of coupled shear walls within a reinforced concrete system is simulated using SeismoStruct software. Material characteristics are established through the Mandler et al [9] model for concrete and a bilinear model is defined for steel reinforcement material. Concrete behavior is represented by inelastic

displacement-based frame elements, while steel coupling beams adopt trilinear spring models. Rigid link constraints are imposed to maintain precise vertical displacement disparity at link element joints. Employing static time history analysis with cyclic displacement records effectively simulates quasi-static cyclic loading. **Fig. 2** shows the modeling conditions of coupled shear walls with steel fuses.

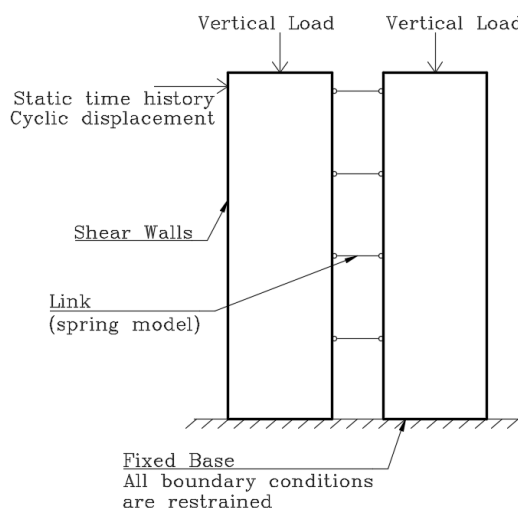


**Fig. 2** Steel Fuse-Coupled Shear Walls Modeling Conditions

## 2.4 Results Analysis

Pushover curves are extracted from ABAQUS FE models to identify the shear parameters of steel beams. Hysteresis curves are extracted from Seismostruct models to determine the full behavior of coupled shear walls (global behavior). Performance criteria feature in Seismostruct is used to determine the damage sequence. This includes minor cracks; identified when concrete wall reaches cracking stress (maximum RC tension strength), longitudinal reinforcement yielding; identified when steel bars reaches yielding strain, RC confined crushing; achieved when concrete stress reaches maximum concrete strength, and RC failure; identified when the structure base shear drops to 85% of the maximum base shear capacity as per James K. Wight [10].

## 3. VERIFICATION

The validation of the proposed modeling methodology relies on benchmarking against previous experimental results. This process is structured into two phases; The first phase involves calibrating micro-modeling of steel fuse beams against experimental tests conducted on replaceable steel beams subjected to cyclic shear loading, while the second phase calibrates macro-modeling for coupled shear walls against experimental tests from literature involving shear walls coupled with conventional concrete beams or replaceable steel beams as fuses.

### 3.1 Phase 1; Replaceable Steel Beams Modeling Calibration

In order to validate steel beams micro-modeling, previous tests were studied and used for this purpose.

Cheng et al. 2021[11] tested a steel H-Built-up section with dimensions 220x8mm for the web, 130x10mm for the flanges, and length of 400mm with two web stiffeners at the two-thirds of its length. The beam was setup vertically between two loading plates, the bottom one is fixed and the upper one is loaded horizontally under shear loading. The test was simulated using ABAQUS FE program with the modeling procedure mentioned in section 2.20. The model showed early yielding for the web of steel fuse beam (weak beam) and this is shown by the stress distribution during shear loading of beam. **Fig. 3** presents a comparison between numerical and experimental pushover curves. It can be observed that the initial stiffness is nearly identical for both curves. The yield shear point is (2.90mm,274kN), and (2.85mm,276kN). The ultimate shear point is (69mm,451kN), and (65mm,454kN) for numerical and experimental results respectively which shows an average error of 3%.

The above presented results show that the prepared FE model reliably represents the steel beams shear behavior and hence can be used to extract the shear behavior of steel beams.

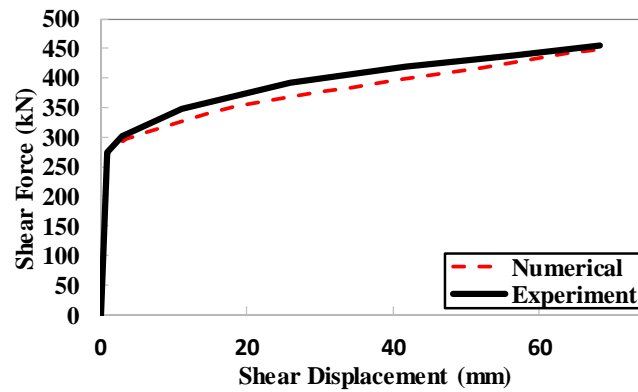
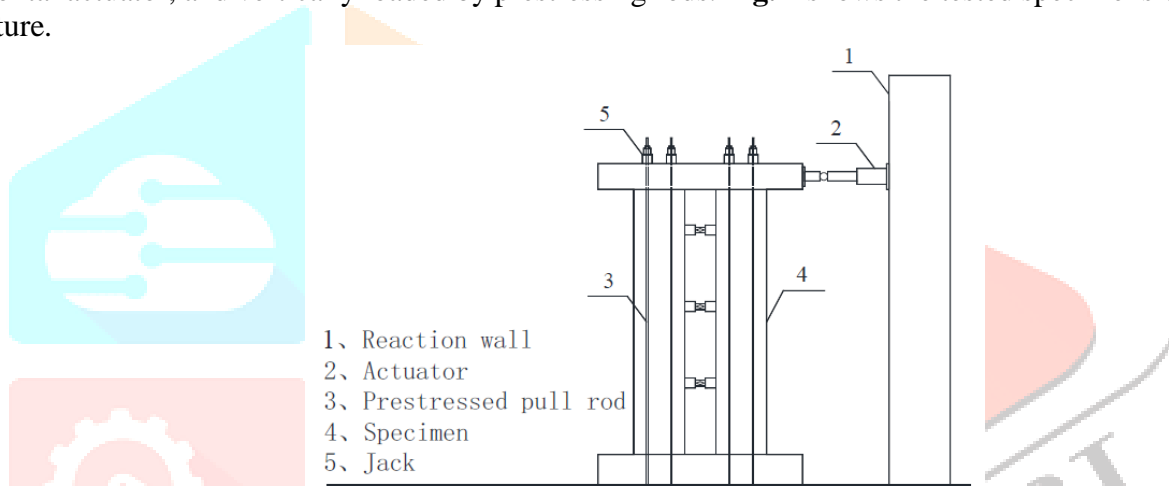


**Fig. 3:** Numerical vs Experiment pushover curve for steel beam

### 3.2 Phase 2; Coupled Shear Walls Modeling Calibration

In order to calibrate FE modeling of global system behavior, Modeling technique mentioned in section 2.30 is used.

Chen et al. 2019 tested three RC coupled shear walls all having the same RC walls dimensions and reinforcement (W1, W2, and W3). Specimens were fixed from bottom and loaded laterally by means of horizontal actuator, and vertically loaded by prestressing rods. **Fig. 4** shows the tested specimens wall setup in literature.



- 1、 Reaction wall
- 2、 Actuator
- 3、 Prestressed pull rod
- 4、 Specimen
- 5、 Jack

**Fig. 4** Tested Specimens wall setup

FE Seismostruct models were conducted to extract hysteresis, skeleton curves, and damage sequence. **Fig. 5, Fig. 6, and Fig. 7** show hysteretic and skeleton curves comparison between numerical and experiment results for W1, W2, and W3 respectively. It should be noted that there was slippage in the positive part of specimen 1 as reported by in literature [4] which resulted in low positive initial stiffness in test results. **Table 1** presents a comparison between numerical and experiment results in terms of stiffness, base shear, and top displacement for specimens 1, 2, and 3. The results show good agreement between the proposed numerical model and the experiment results.

Regarding damage sequence of W1, RC coupling beams experienced cracking at wall top displacement of 8mm, and 6mm in experiment and FE model respectively. Also, the wall base suffered cracking at wall top displacement of 40mm, and 42mm in experiment and FE model respectively. As for W2, steel coupling beams yielded at wall top displacement of 40mm, and 30mm in experiment and FE model respectively. Also, Wall base cracking happened at wall top displacement of 50mm, and 60mm in experiment and FE model respectively. Damage sequence for W3 was not available in literature. **Table 2** presents the damage sequence of the tested specimens and the numerical models for the three specimens. Based on the results, the numerical model shows good agreement with the experimental results.

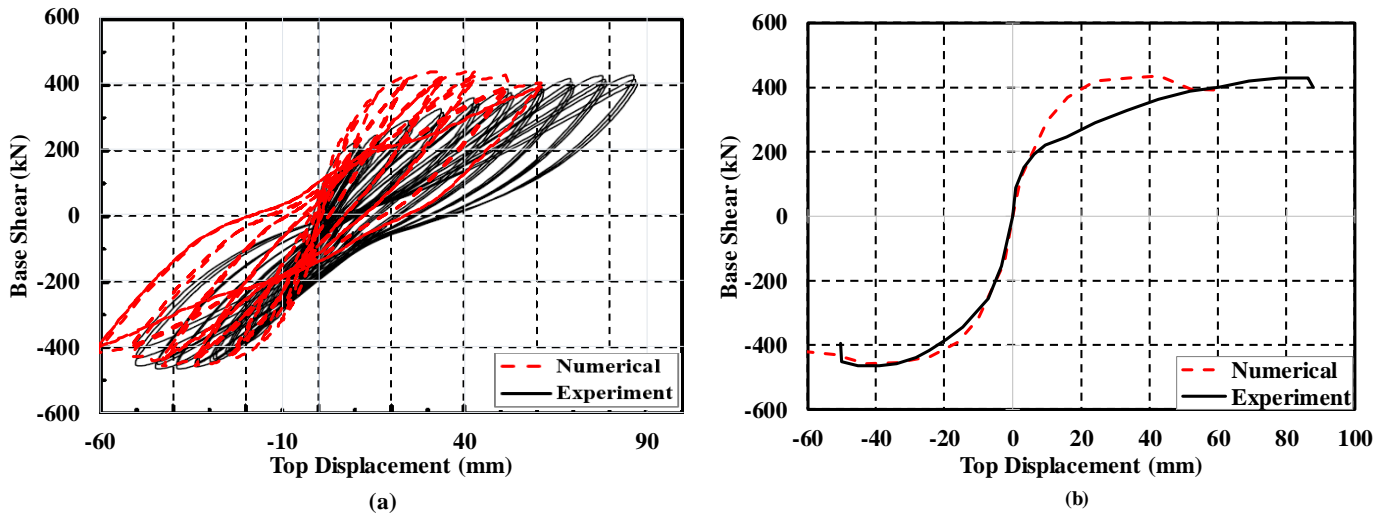


Fig. 5: Numerical vs Experiment hysteretic/skeleton curves for W1; (a) Hysteresis curve for W1, (b) Skeleton curve for W1.

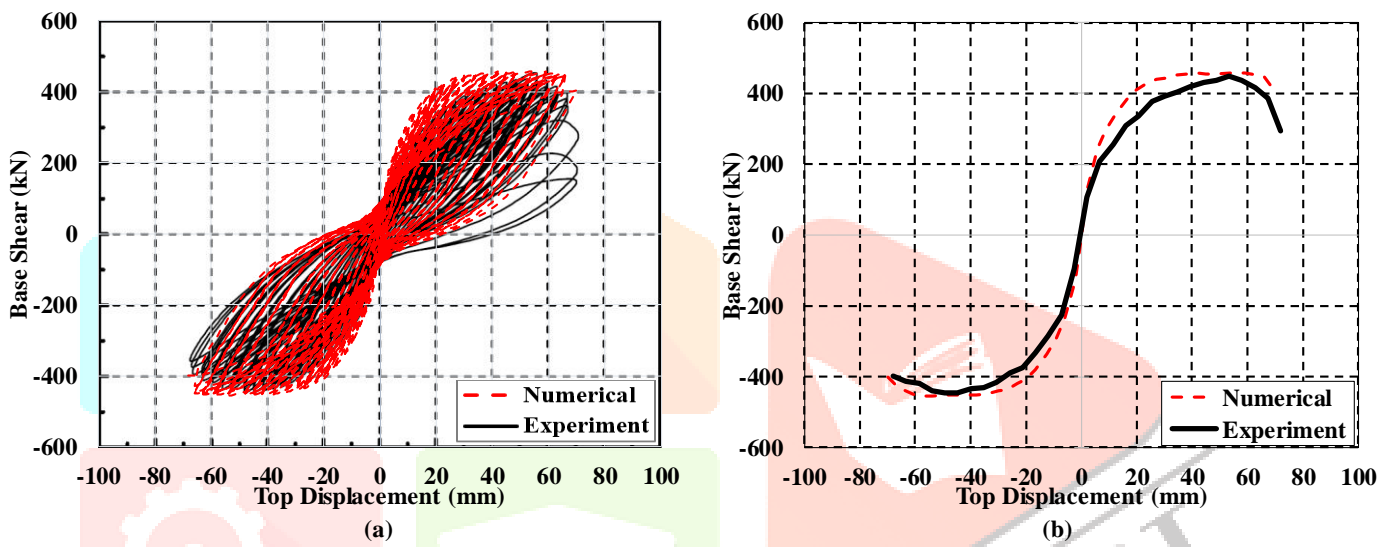


Fig. 6: Numerical vs Experiment hysteretic/skeleton curves for W2; (a) Hysteresis curve for W1, (b) Skeleton curve for W2.

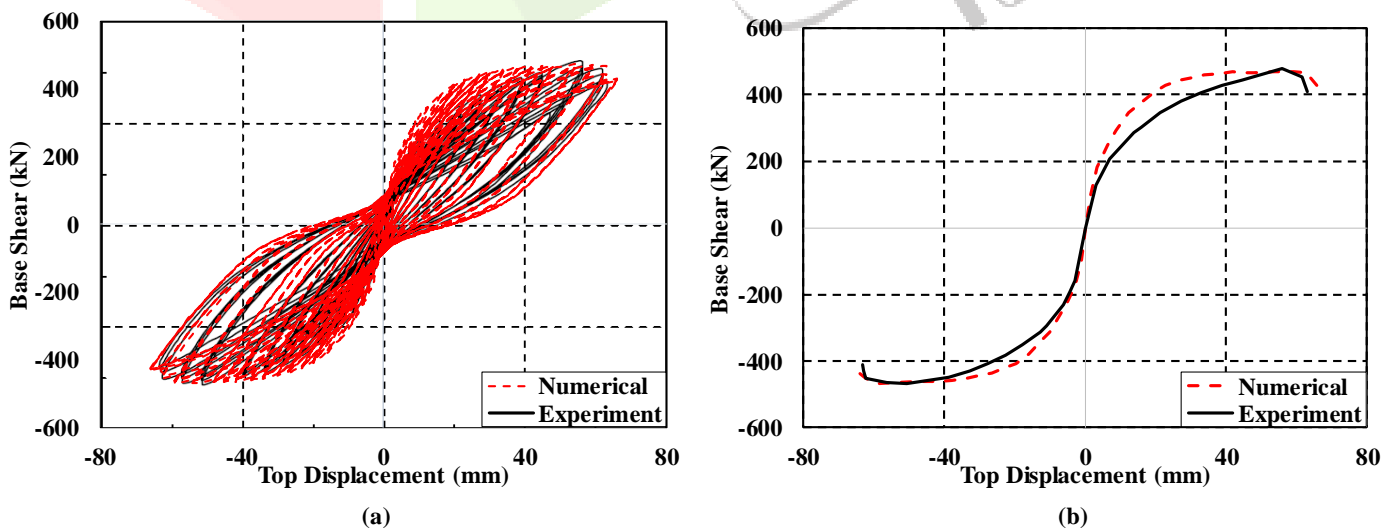


Fig. 7: Numerical vs Experiment hysteretic/skeleton curves for W3; (a) Hysteresis curve for W1, (b) Skeleton curve for W3.

**Table 1:** Yun Chen Experiments vs FE Models Results

Behavior Parameter	Specimen (1)			Specimen (2)			Specimen (3)		
	Exp.	FE	Exp/F E	Exp	FE	Exp/F E	Ex p.	FE	Exp/F E
Initial Stiffness (kN/mm)	34	39	0.87	33	38	0.87	58	63	0.92
Peak Base Shear (kN)	464	45 7	1.01	448	454	0.99	484	47 3	1.02
Peak Top Displacement (mm)	44	43	1.02	50	54	0.93	55	54	1.02

**Table 2:** Experiment vs Numerical Top Displacement (mm) at Control Damage States

Damage State	Specimen 1		Specimen 2		Specimen 3	
	Test	Numerical	Test	Numerical	Test	Numerical
RC beam cracking	8	6	N/A	N/A	N/A	N/A
Fuse yield	N/A	N/A	40	30	*	42
Wall base cracking	40	42	50	60	*	63

\*Data missing from literature

#### 4. PARAMETRIC STUDY

Using the presented modeling technique, the verified models are then implemented to carry out an extensive parametric study. The study aims at investigating several parameters to improve the micro and macro behavior of the system in terms of energy dissipation, damage probability at different drift levels, and maintain the strength of the proposed system. The parametric study is divided into two phases; phase one is to determine the effective steel fuse dimensions ratio for an ordinary H-built-up steel section with web stiffeners. While phase two is meant to study the effect of replacing the conventional RC coupling beams with steel coupling beams according to recommendations concluded from phase one.

##### 4.1 Phase One

H-Built-up steel beam section is studied to determine the optimum dimensions of the steel beam according to the given beam length and the required shear capacity which guarantee ductile shear behavior of the steel fuse beam. As shown in **Table 3**, five different cross sections named S1, S2, S3, S4, and S5 are modelled in ABAQUS FE model with nine different beam clear lengths. Each length has a different value of " $e/(M_p/V_p)$ " with a range from 0.95 to 1.95. The beam clear lengths are chosen to guarantee shear yielding instead of flexural yielding according to AISC-seismic-2010 [12] which ensures that the plastic shear capacity of steel beams depends on cross section dimensions and material only. Hence,  $M_p$  and  $V_p$  are fixed values for each specimen while changing the clear length of the beam. The steel beam flanges, and web dimensions are chosen to satisfy the slenderness limits of Table D1.1 in AISC-seismic-2010 [12] for highly ductile members.

$e$  = link length

$M_p$  = nominal plastic flexural strength =  $f_y * Z_x$

$V_p$  = nominal shear strength of an active link =  $0.60 * A_{web} * h_{web} * f_y$  (in case of shear yielding)

$V_p = 2M_p/e$  (in case of flexural yielding)

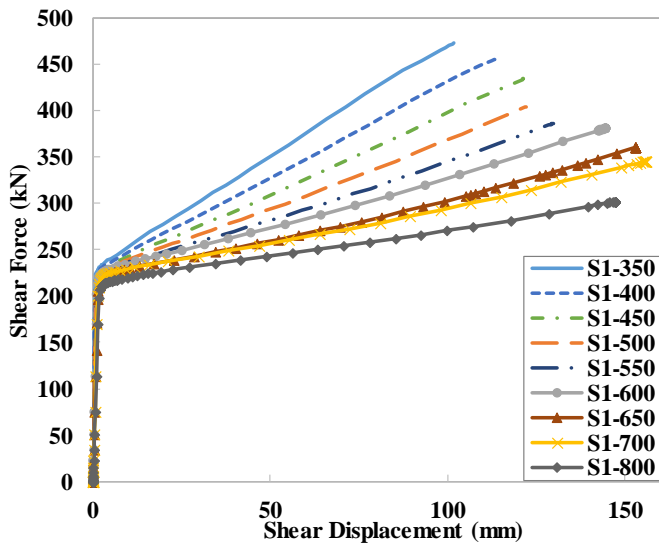
**Table 3:** Steel fuse dimensions

Specimen	$h_w$	$t_w$	$b_f$	$t_f$
S1	240	8	120	12
S2	210	6	90	9
S3	300	10	140	14
S4	270	8	120	10
S5	290	9	120	12

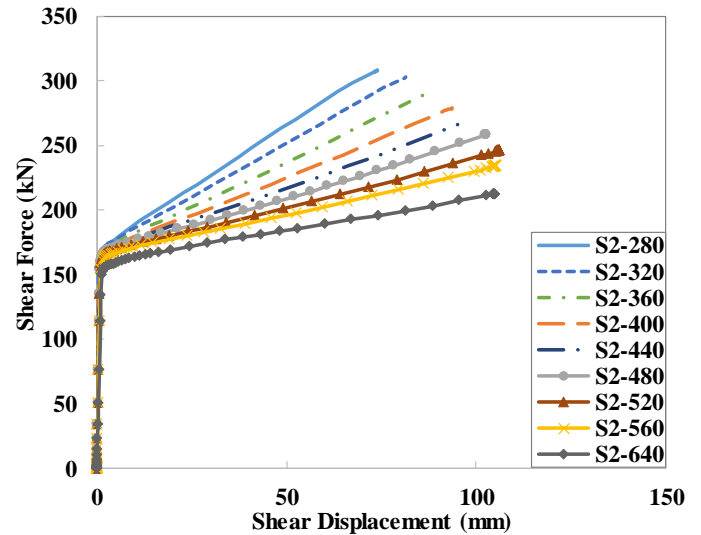
This parametric study aims at determining the optimum steel beam dimensions to achieve the best energy absorption, and deformation capacity at different shear capacity levels. Each specimen is shear loaded in ABAQUS FE model with the same procedures explained in the verification sections. Pushover curves are extracted for each of the above-mentioned specimens as shown in **Fig. 8**. Each specimen in the figure is defined by its name and length, for example "S1-length in mm". It can be noted that the deformation (shear rotation) capacity increases with increasing specimen length until the factor " $e/(M_p/V_p)$ " reaches a value of

1.69 approximately. Then, the deformation and shear capacity, and yielding shear force starts to decrease until a ratio of 2.00 which indicates the end of shear yielding behavior and beginning of flexural yielding phase which is not preferred as shear yielding guarantees a larger yielding area (the whole web) than of flexural yielding (ends of beam flange), which means larger energy dissipation. Additionally, it is noticed that at low ratios, the steel beams failed at relatively limited deformations which indicates brittle behavior and low energy dissipation. **Fig. 9** shows the relation between maximum shear displacement, shear capacity, and energy absorbed against “ $e/(M_p/V_p)$ ” value for the above-mentioned steel beams. It should be noted that  $M_p/V_p$  is a constant value for each cross section, and the variable parameter is the beam length ( $e$ ).

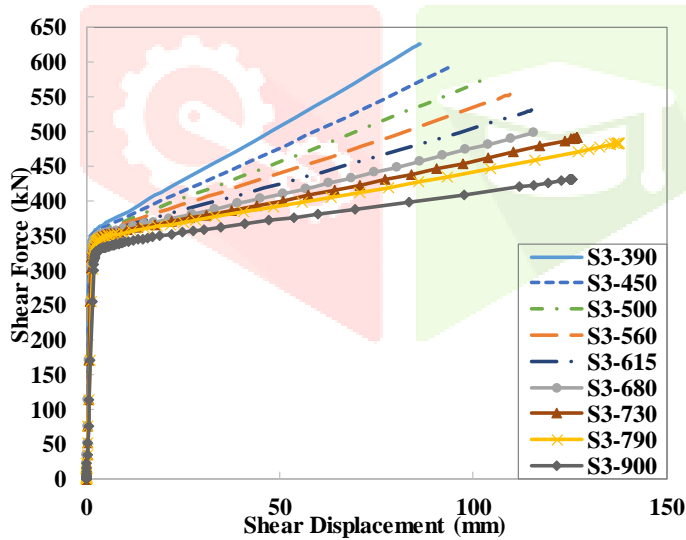
From These figures, the optimum ratio of “ $e/(M_p/V_p)$ ” is determined to range from 1.55 to 1.69. This range ensures maximum shear deformation capacity and energy absorption while maintaining reasonable shear capacity.



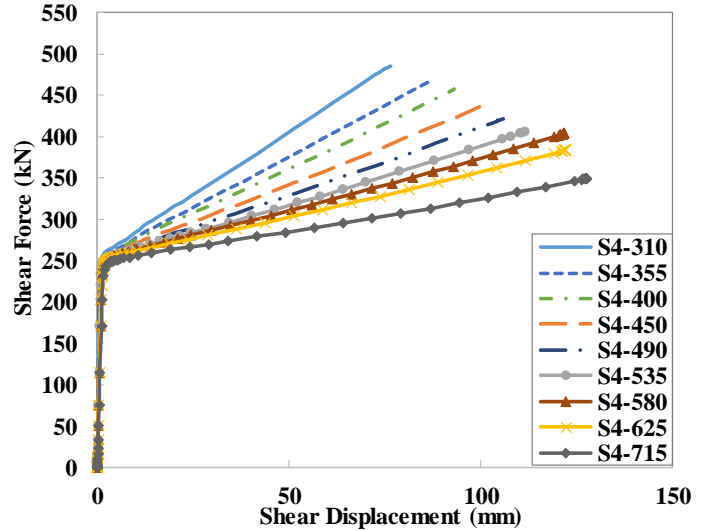
(a) Skeleton curves for S1 specimens



(b) Skeleton curves for S2 specimens



(c) Skeleton curves for S3 specimens



(d) Skeleton curves for S4 specimens

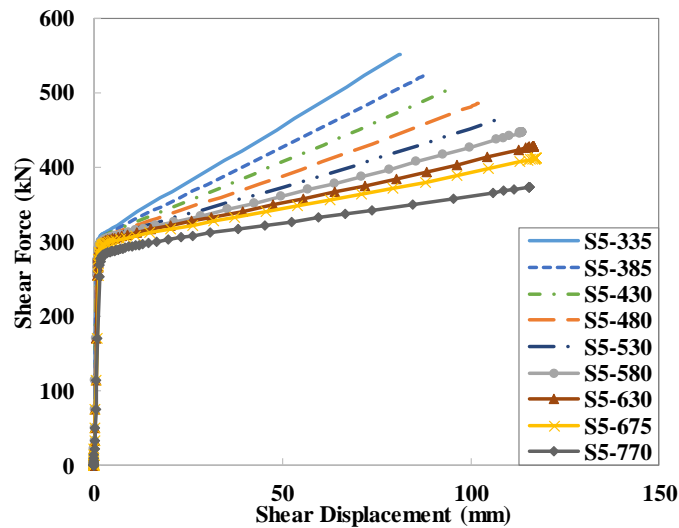


**Fig. 8:** Shear-Displacement curves for S1:S5 specimens; (a) Pushover curves for S1 specimens, (b) Pushover curves for S2 specimens, (c) Pushover curves for S3 specimens, (d) Pushover curves for S4 specimens, (e) Pushover curves for S5 specimens.

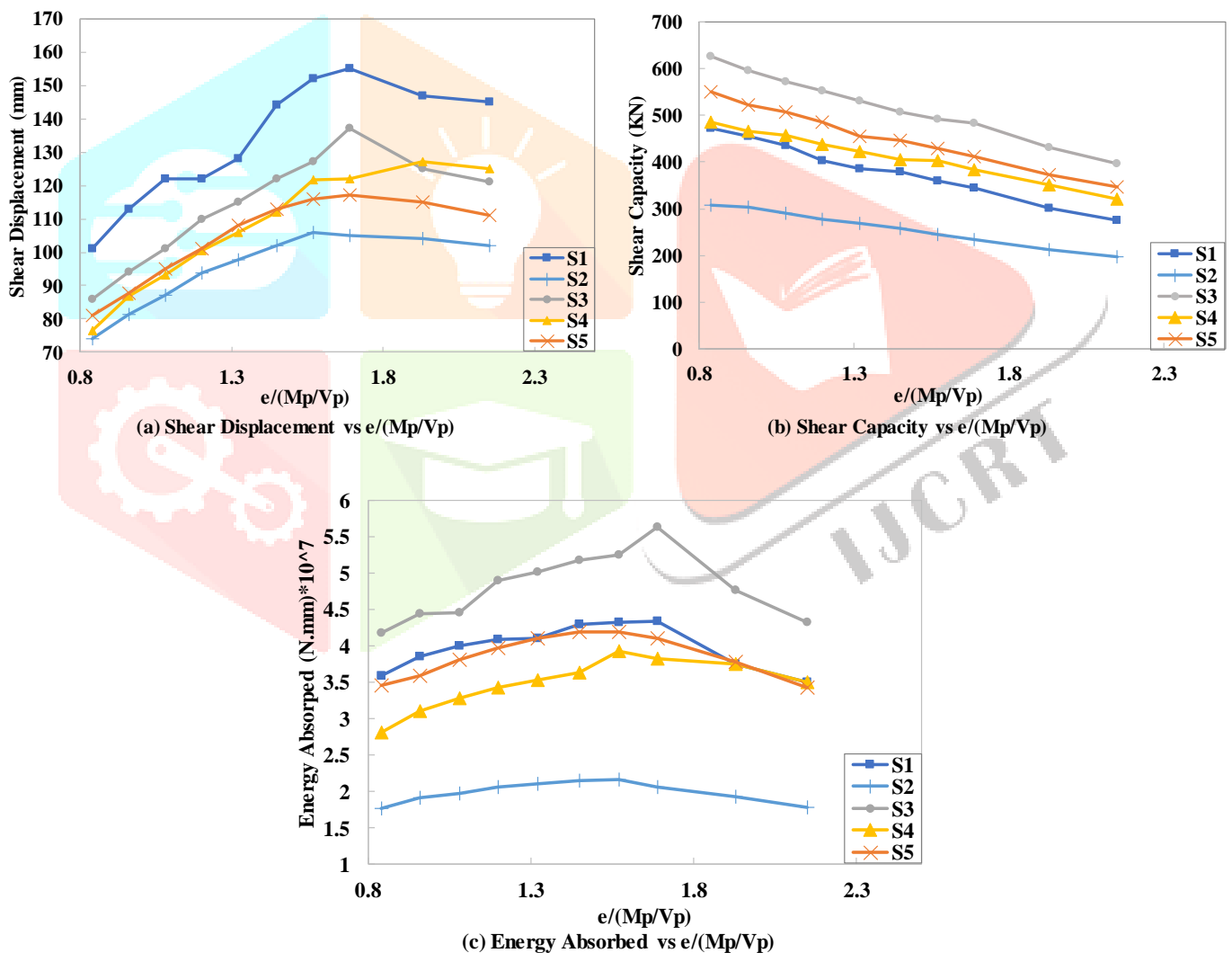


**Fig. 9:** (a) Shear Displacement vs “ $e/(M_p/V_p)$ ” ratio, (b) Shear Capacity vs “ $e/(M_p/V_p)$ ” ratio, (c) Energy Absorbed vs “ $e/(M_p/V_p)$ ” ratio.



### 4.2 Phase two

The purpose of this phase is to study the global behavior of coupled shear walls while using conventional concrete coupling beams against replaceable steel BUS coupling beams (S1-S5). A four-story twin shear walls 1300x200mm (W1) with 1500mm story height is studied. The clear distance between the two walls equals the length of the used steel beams. The wall is laterally loaded from the top by cyclic loading with a number of 3 cycles at each displacement step until a drift of 2.80% or reaching the ultimate base shear which is defined as 85% of the max base shear capacity reached by the analyzed system. **Fig. 10** shows the details of the studied structure in this phase. Five different shear walls are analyzed while coupled with the previously mentioned steel fuses S1-S5 having the previously identified optimum ratio of “ $e/(M_p/V_p)$ ” =1.60. Additionally, five identical models are studied while coupled with RC beams named C1:C5 shown in **Table 4** having the same shear yielding capacity as the steel fuses S1:S5 respectively.

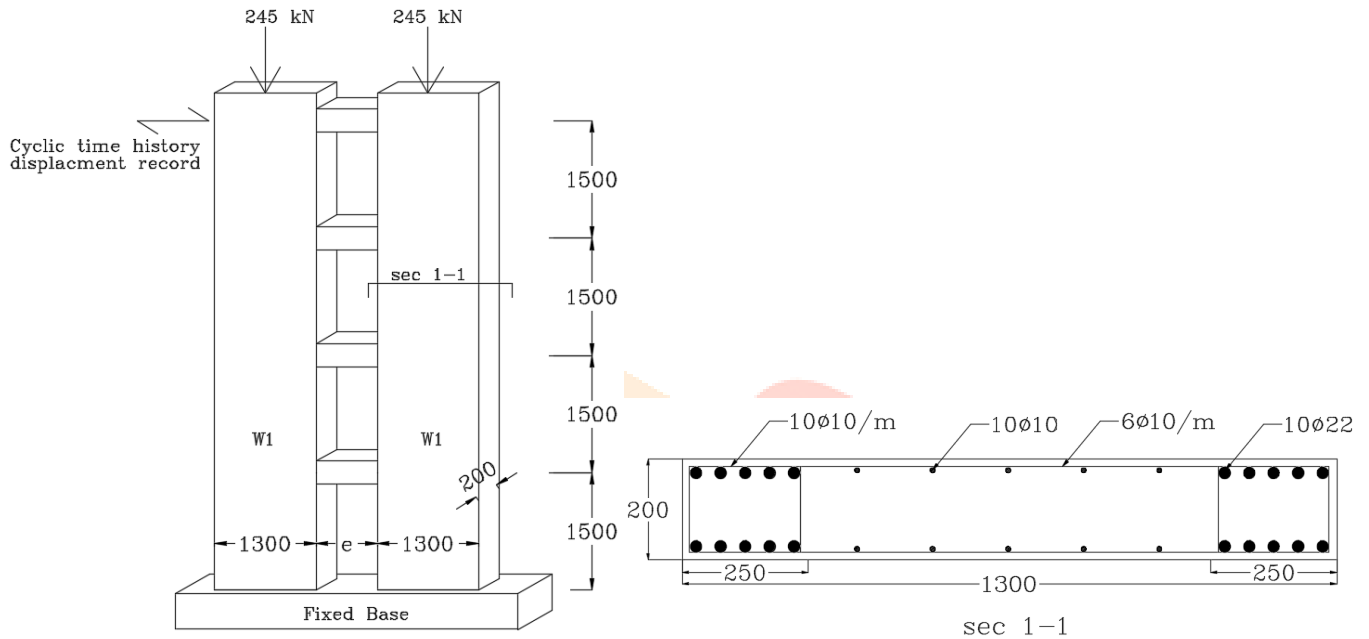


**Fig. 10** Dimension and Reinforcement details of W1

**Table 4:** Concrete coupling beams details

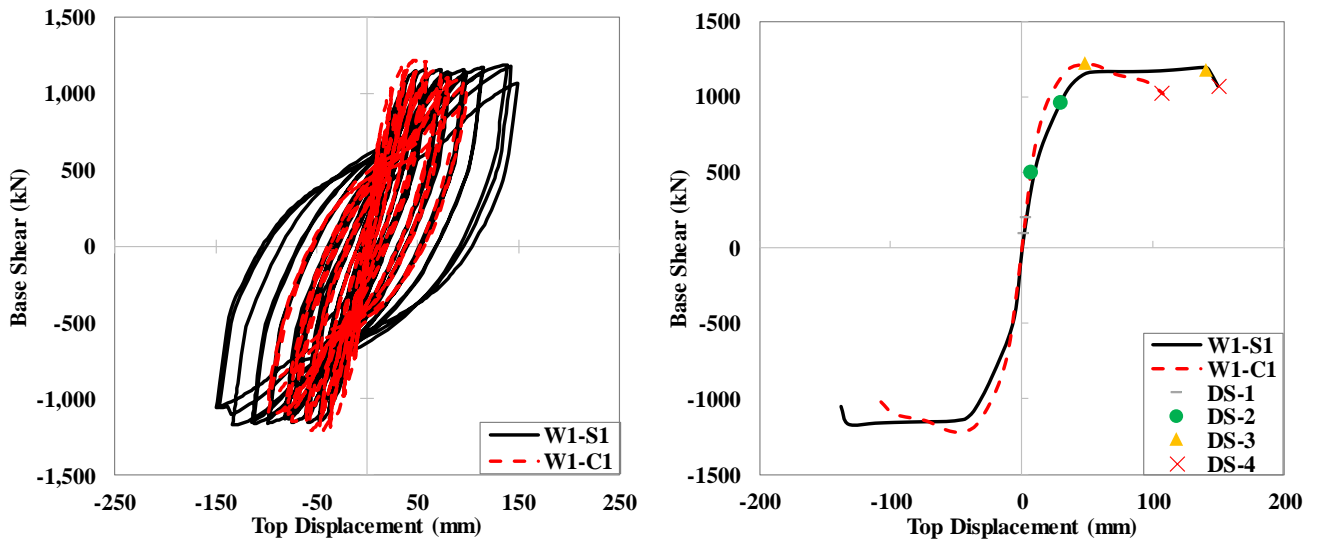
Concrete Beam	Width (mm)	Depth (mm)	Longitudinal Reinforcement	Stirrups	Length (mm)
C1	200	300	6φ10	10φ10/m	650
C2	200	250	6φ10	10φ8/m	520
C3	250	400	6φ10	10φ10/m	790
C4	250	300	6φ10	10φ8/m	580
C5	250	350	6φ10	10φ10/m	630

Hysteresis and backbone curves for each of the ten specimens are extracted from the FE model and are presented in **Fig. 11** to **Fig. 15**. Each figure shows comparison between specimens having RC and steel coupling beam with the same shear capacity, where damage states indicated in the mentioned figures are defined as:

- DS-1: minor cracking (RC stress reaches  $F_{ctr}$ )
- DS-2: Longitudinal reinforcement yield (steel bars stress reaches  $F_y$ )
- DS-3: RC confined crushing (RC stress reach  $F_{cu-confined}$ )
- DS-4: Base shear reaches 85% of maximum base shear.

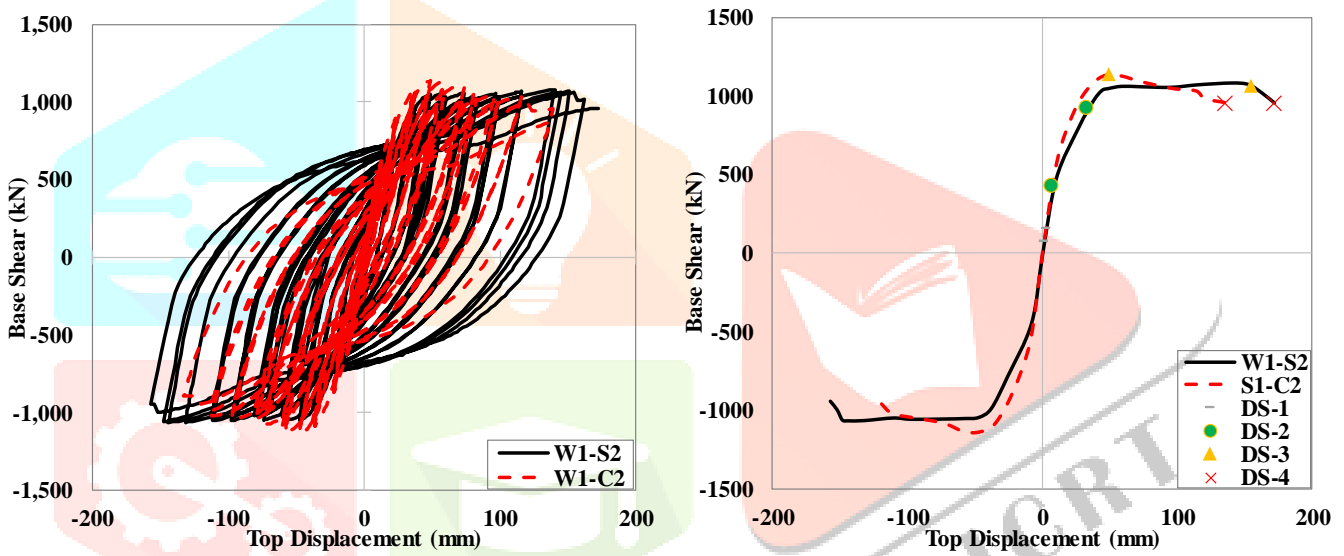
From these figures, steel fuse coupling beam showed (in comparison with RC coupling beams) increased drift at DS-2 from 0.10% to 0.41% , at DS-3 by an average of 291%, and at DS-4 by an average of 47%. The ductility of the system increased by 34%. The maximum energy dissipation increased by 40%. The initial stiffness decreased to 60%, while the maximum base shear is nearly the same. The concrete coupling beams failed at an average top drift of 0.34% before walls cracking at 0.86% drift, while steel fuse beams yielded at earlier stage, but kept its strength until failure of the RC walls at top drift of about 2% increasing the

system deformation capacity. It should be noted that steel beams can be replaced after yielding due to earthquake considering bolted connections with shear walls.



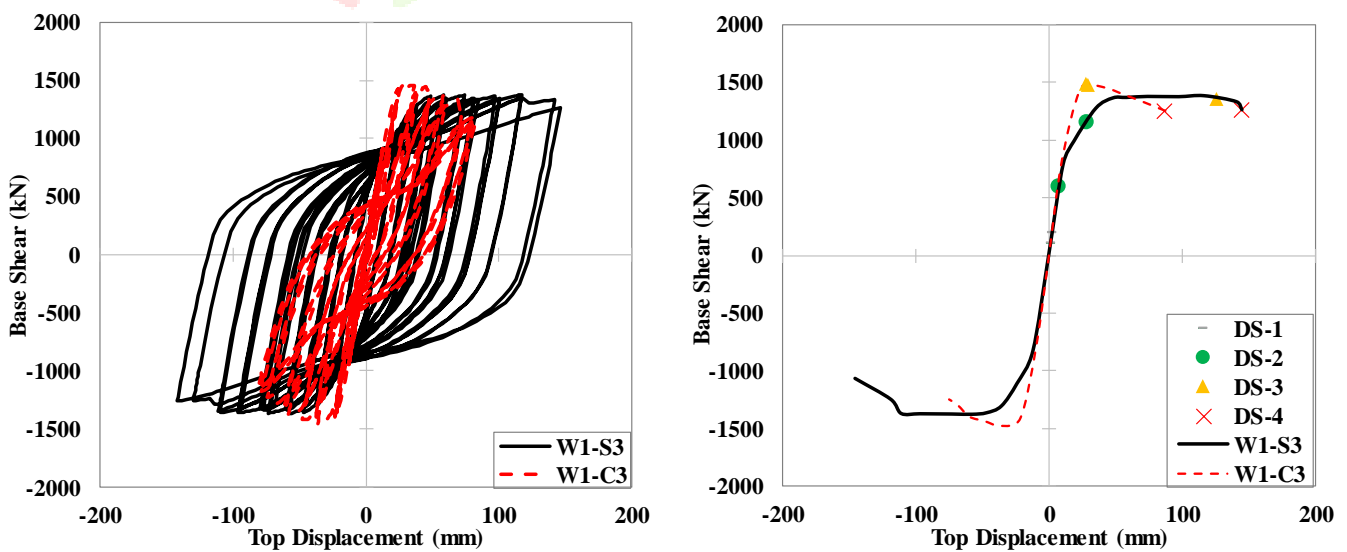
(a) Hysteresis Curve for W1-S1 vs W1-C1 (b) Skeleton Curve for W1-S1 vs W1-C1

**Fig. 11:** W1-C1 vs W1-S1; (a) Hysteretic Curves, (b) Skeleton Curves.



(a) Hysteresis Curve for W1-S2 vs W1-C2 (b) Skeleton Curve for W1-S2 vs W1-C2

**Fig. 12:** W1-C2 vs W1-S2; (a) Hysteretic Curves, (b) Skeleton Curves.



(a) Hysteresis Curve for W1-S3 vs W1-C3 (b) Skeleton Curve for W1-S3 vs W1-C3

**Fig. 13:** W1-C3 vs W1-S3; (a) Hysteretic Curves, (b) Skeleton Curves.

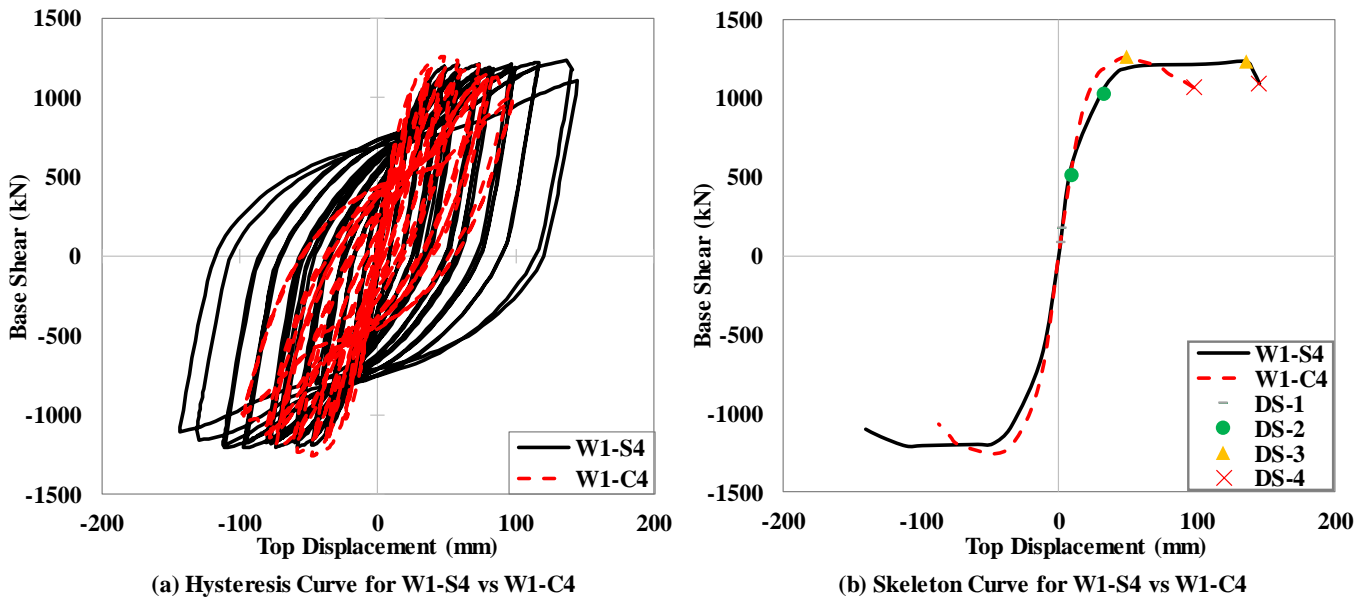


Fig. 14: W1-C4 vs W1-S4; (a) Hysteretic Curves, (b) Skeleton Curves.

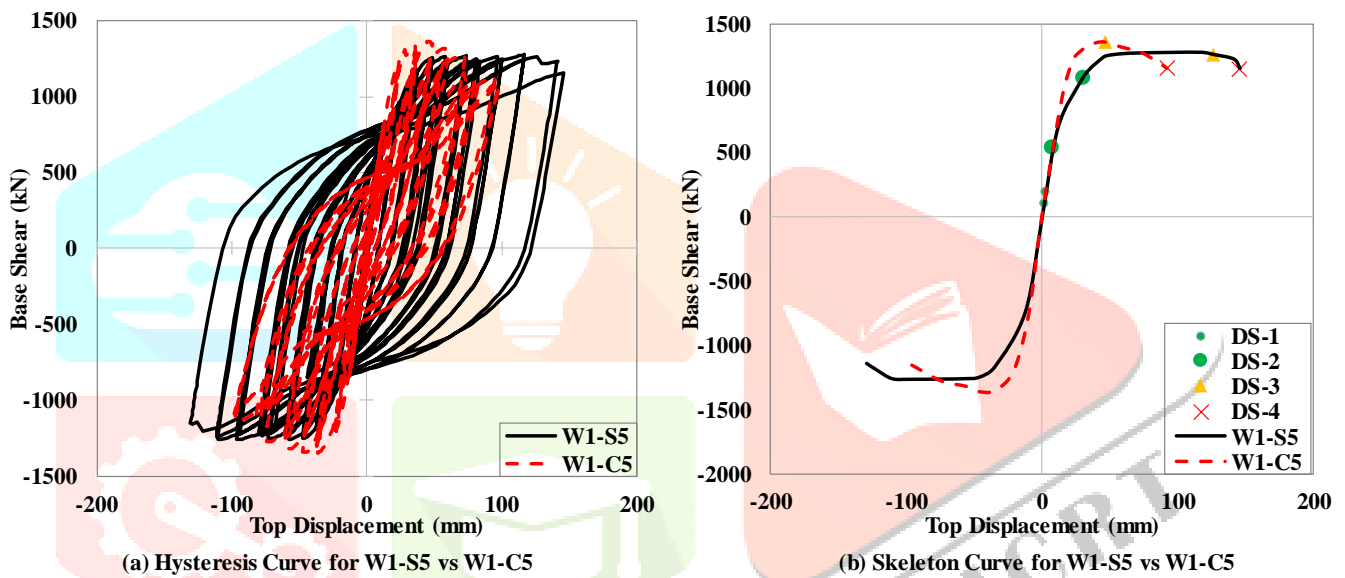


Fig. 15: W1-C5 vs W1-S5; (a) Hysteretic Curves, (b) Skeleton Curves.

### 5.CONCLUSIONS

- Steel beams of built-up sections gives optimum shear behavior in terms of energy dissipation, and displacement capacity when the factor " $\frac{e}{M_p/V_p}$ " ranges from 1.55 to 1.69.
  - Steel beams of built-up sections guarantees shear yielding under shear loading when the factor " $\frac{e}{M_p/V_p}$ " is less than 2.0 and suffers flexural yielding when the mentioned factor reaches or exceeds a value of 2.0.
  - Steel beams of built-up sections which are governed by web shear yielding dissipates more energy than those governed by flexural yielding under shear loading due to yielding of a larger area.
  - Steel coupling beams with specific dimensions recommended in this research is considered a better alternative overconventional concrete coupling beams. As the steel coupling beams can result in increasing deformation capacity by 47%, and the energy dissipation by 40% for the main system while maintaining the same base shear capacity.
  - Steel coupling beams result in low initial stiffness of the whole system which may result in non-structural damage of ordinary buildings. Hence, this system should be checked against drift limits in design codes and is preferred to be used in structures that may not experience this type of damage as bridges and factories.
- Steel coupling beams can be easily replaced after yielding due to seismic activity while maintaining the building serviceability.

## 6. REFERENCES

- [1] Popov, E. P., Takanashi, K., & Roeder, C. W. (1976). Structural steel bracing systems: Behavior under cyclic loading. Earthquake Engineering Research Center, College of Engineering, University of California.
- [2] Fintel, M., & Ghosh, S. K. (1977, July). STRUCTURAL SYSTEMS FOR EARTHQUAKE RESISTANT CONCRETE BUILDINGS. In Proceedings of the Workshop on Earthquake-Resistant Reinforced Concrete Building Construction, University of California, Berkeley (pp. 707-741).
- [3] Fortney, P. J., Shahrooz, B. M., & Rassati, G. A. (2007). Large-scale testing of a replaceable “fuse” steel coupling beam. *Journal of structural engineering*, 133(12), 1801-1807.
- [4] Lu, X., Chen, Y., & Jiang, H. (2018). Earthquake resilience of reinforced concrete structural walls with replaceable “fuses”. *Journal of Earthquake Engineering*, 22(5), 801-825.
- [5] Cheng, M. Y., Fikri, R., & Chen, C. C. (2015). Experimental study of reinforced concrete and hybrid coupled shear wall systems. *Engineering Structures*, 82, 214-225.
- [6] Li, G. Q., Pang, M. D., Li, Y. W., Li, L. L., Sun, F. F., & Sun, J. Y. (2019). Experimental comparative study of coupled shear wall systems with steel and reinforced concrete link beams. *The Structural Design of Tall and Special Buildings*, 28(18), e1678.
- [7] “Abaqus/CAE User’s Manual Abaqus 6.11 Abaqus/CAE User’s Manual.”
- [8] “SeismoStruct User Manual,” 2002. [Online]. Available: <https://seismosoft.com/>.
- [9] Mander, J. B., Priestley, M. J., & Park, R. (1988). Theoretical stress-strain model for confined concrete. *Journal of structural engineering*, 114(8), 1804-1826.
- [10] MacGregor, J. G., Wight, J. K., Teng, S., & Irawan, P. (1997). Reinforced concrete: Mechanics and design (Vol. 3). Upper Saddle River, NJ: Prentice Hall.
- [11] Cheng, Q., Lian, M., Su, M., & Zhang, H. (2021, February). Experimental and finite element study of high-strength steel framed-tube structures with replaceable shear links under cyclic loading. In *Structures* (Vol. 29, pp. 48-64). Elsevier.
- [12] AISC (American Institute of Steel Construction). (2010). Seismic provisions for structural steel buildings. Chicago: AISC.

